Environmental Earth Sciences (2018) 77:625
https://doi.org/10.1007/s12665-018-7807-6

ORIGINAL ARTICLE

Magnetic tracing of sediment dynamics of mudbanks off southwest coast of India

F. Badesab[1] · V. Gaikwad[1] · T. R. Gireeshkumar[2] · O. Naikgaonkar[1] · K. Deenadayalan[3] · S. V. Samiksha[1] · P. K. Dinesh Kumar[2] · V. J. Loveson[1] · S. D. Iyer[1] · A. Khan[1] · P. B. Udayakrishnan[1] · A. Sardar[1]

Received: 8 June 2018 / Accepted: 1 September 2018 / Published online: 8 September 2018

Abstract

In this study, we utilized environmental magnetic in combination with sedimentological and hydrodynamic data to investigate the formative processes of mudbanks along southwest coast of India. We document the linkages between enrichment of silt-sized magnetic particles and formation processes of mudbanks along Alappuzha coast. A trend of increasing magnetite concentration and coarsening in magnetic grain size is observed at mudbank stations M2 and M3, while the mud-deficient station (M1) showed an opposite trend. A strong relationship between magnetic and physical grain size for all samples implies that the magnetic particle size and clastic grain size are largely adjunct. Analysis of rock magnetic and grain size data of surficial and suspended sediments from non-mudbank (M1) and two mudbank stations (M2, M3) reflect the differential sediment partitioning and transport regimes which controlled the formation of mudbanks along Alappuzha coast. Two plausible mechanisms responsible for the formation of mudbanks are identified: grain size-selective entrainment is the dominant process during pre-monsoon; weaker hydrodynamics (waves and bottom currents) favors accumulation of silt-sized (fine and coarse) magnetic and non-magnetic fractions resulting in the formation of magnetically low-enriched sediment bed of mixed grain sizes. At the onset of monsoon, wave-induced energetic bottom currents enhance the suspension of entire sediment bedload at stations M2, M3 to form fluid mud. Concurrently, mineral-density-based selective fractionation allows the settling of coarse silt-sized magnetic particles, while the fine magnetic silt-size particles accumulate forming thick fluid mud as a suspension load resulting in the formation of mudbanks. An observed increase in magnetic susceptibility and coarsening in magnetic grain size of surficial sediments at mudbank stations (M2, M3) during monsoon period supports the interpretation. Our findings are summarized in a conceptual model which can be very well applied to investigate sediment dynamics associated with mudbank formation in coastal and shelf sedimentary systems.

Keywords Environmental magnetism · Mudbanks · Sediment dynamics · Magnetic susceptibility · Grain size

Introduction

Mudbanks are calmer regions with turbid waters carrying huge loads of suspended sediments and are formed as a result of suspension and deposition of mud in the coastal regions, especially during monsoon. Coastal morphology, sediment supply from fluvial and marine sources, depositional environment and prevailing hydrodynamics play an important role in formation and occurrences of mudbanks in coastal systems (Froidefond et al. 1988; Mehta 2002; Allison and Lee 2004; Anthony et al. 2002, 2010). Mudbanks have been reported to occur close to the river embayment, which receives higher supply of mud from the fluvial sources especially during monsoon. Examples of such river-induced mudbanks include: Mississippi Chenier coast (McBride et al. 2007), Amazon coast (Anthony et al. 2007), Mekong delta coast (Tamura et al. 2010), Florida Bay, Louisiana coast (Wells and Roberts 1980a, b; McBride et al. 2007), Gulf of Papua (Walsh and Nittrouer 2004) and northeast coast of Brazil and China (Allison et al. 2000; Liu et al. 2006).

✉ F. Badesab
firoz@nio.org

[1] CSIR, National Institute of Oceanography, Dona Paula, Goa 403004, India

[2] CSIR, National Institute of Oceanography, Regional Centre, Kochi, Kerala 682018, India

[3] Indian Institute of Geomagnetism, New Panvel, Navi Mumbai, Maharashtra 410218, India

The mudbanks off Alappuzha are unique as they occur in a non-estuarine region as a temporary feature only during monsoon along the southwest coast of India. There is no major river system feeding the mud to this particular coastal stretch off Alappuzha unlike other well-reported sites having permanent mudbanks formed as a result of higher mud supply from river runoff; for example, Guyana coast related to the Amazon River (Eisma and Van der Marel 1971) and the inner shelves of Suriname River (Rine and Ginsburg 1978, 1985; Wells et al. 1978; Wells and Coleman 1981a, b) and Louisiana (Wells and Roberts 1980a, b). The mudbanks off Alappuzha are a socio-economically important region for the country and have gained nationwide attention because of the generation of a calm environment with high biological productivity which facilitates intense fishing activities and acts as a natural barrier against energetic monsoonal waves and prevents coastal erosion (Gopinathan and Qasim 1974; Nair et al. 1984; Thompson 1986). Previously, several researchers have attempted to decipher the formative mechanism of mudbanks and various plausible hypotheses have been proposed, including coastal upwelling (Ramasastry and Myrland 1959; Karnan et al. 2017; Gireeshkumar et al. 2017), transport of suspended sediments by littoral and rip currents (Varma and Kurup 1969; Kurup 1977; Shynu et al. 2017), wave-induced oscillations and dampening (MacPherson and Kurup 1981; Mathew 1992), infra-gravity waves (Tatavarti et al. 1996, 1999; Tatavarti and Narayana 2006), flows of mud from terrestrial sources to sea through subterranean channel network. Crawford (1860), Menon (1924), King (1881), Jacob et al. (2015) and Loveson et al. (2016) argued over the validity of subterranean conduit flow of mud/water from the Vembanad Lagoon, (Bristow 1938; Balachandran 2004), seepage of methane gas due to injection of freshwater from the lagoon (Narayana et al. 2008), fluctuations in short-period storm waves during monsoon (Nair 1976), existence of submerged trending faults (Mallik et al. 1988), bottom salinity variations (Mallik et al. 1988; Mathew and Gopinathan 2000; Balachandran 2004; Nair et al. 2013), hydrocarbon explosion (Nair 1976; Narayana et al. 2008) and supply of mud from offshore region to the coast through depression channel network (Muraleedharan et al. 2017). However, the formative mechanism concentrating the localized mud as temporary mudbanks during monsoon period and stills remains as enigma.

Magnetic minerals are ubiquitous in coastal and shelf systems and are sensitive to environmental conditions (Thompson and Oldfield 1986; Maher and Thompson 1999; Evans and Heller 2003). The entrainment, fractionation, enrichment and transport of magnetic particles are controlled by the complex interaction between coastal morphology and prevailing hydro-sediment dynamics, while sediment provenance decides on the magnetic mineralogy (Rao 1957; Slingerland 1977; Komar and Wang 1984; Frihy and Dewidar 2003; Gallaway et al. 2012). Environmental magnetic method has been widely applied to characterize the fluvial, estuarine, nearshore and marine sediments and can provide information on the sediment sources, transport dynamics and depositional environments (Oldfield et al. 1985; Foster et al. 1991; Hatfield and Maher 2008; Cioppa et al. 2010; Zhang et al. 2010). So far, only a few attempts have been made in the past to explore the potential of environmental magnetic methods to investigate the processes associated with the formation of mudbanks along Alappuzha Coast. Considering the magnetic perspectives, the present study utilizes application of environmental magnetism in combination with sedimentological and hydrodynamic data to magnetically track the physical and sedimentary processes (entrainment, transport, sorting, settling, and enrichment of mud) associated with the formation of mudbanks.

Study area

Location, geology and hydrodynamics of Alappuzha region

The study area is located along the southwest coast of India in Alappuzha district of Kerala state (Fig. 1). The geology of the study area is dominated by Tertiary and Quaternary sedimentary formations, which overlie on the Precambrian gneissic basement rocks (GSI, 1979). The Quaternary sediments comprise of coastal and riverine alluvium overlaying the laterite followed by semi-consolidated to consolidate Tertiary sediments of Warkali (Lower Miocene), Quilon (Lower Miocene) and Vaikom (Oligocene to Eocene) formation in succession. The alluvial deposits consist of clays, sands, shell deposits and terrigenous sands. An activated trending fault extends to the coastal sedimentary basins and the areas of mudbanks lies proximal to this major submerged extension of NE–SW- and NW–SE-oriented continental structural lineaments (Varadarajan and Balakrishnan 1980; Mallik et al. 1988; Padmalal et al. 2014). Continental shelf region of Kerala is formed as a result of faulting during late Pliocene (Krishnan 1968). Numerous rivers and streams pass through lagoons and backwaters and supplies sediment load to the sea.

The shelf off Alappuzha region is narrow and beach ridge exist in the water depth of about 20 m. The shelf gradient is gentle and isobaths of 10 m and 20 m are at about 5 km and 10 km distance from the shore (Narayana et al. 2008). The coast experiences microtidal environment having semidiurnal tides which ranges less than 1 m. The tidal currents are not significant in Alappuzha region. The continental slope is uniformly gentle ($<1°$) towards the sea and attains a water depth of about 9–10 m and 4–5 km from the shore. Around 70% of the annual rainfall occurs during

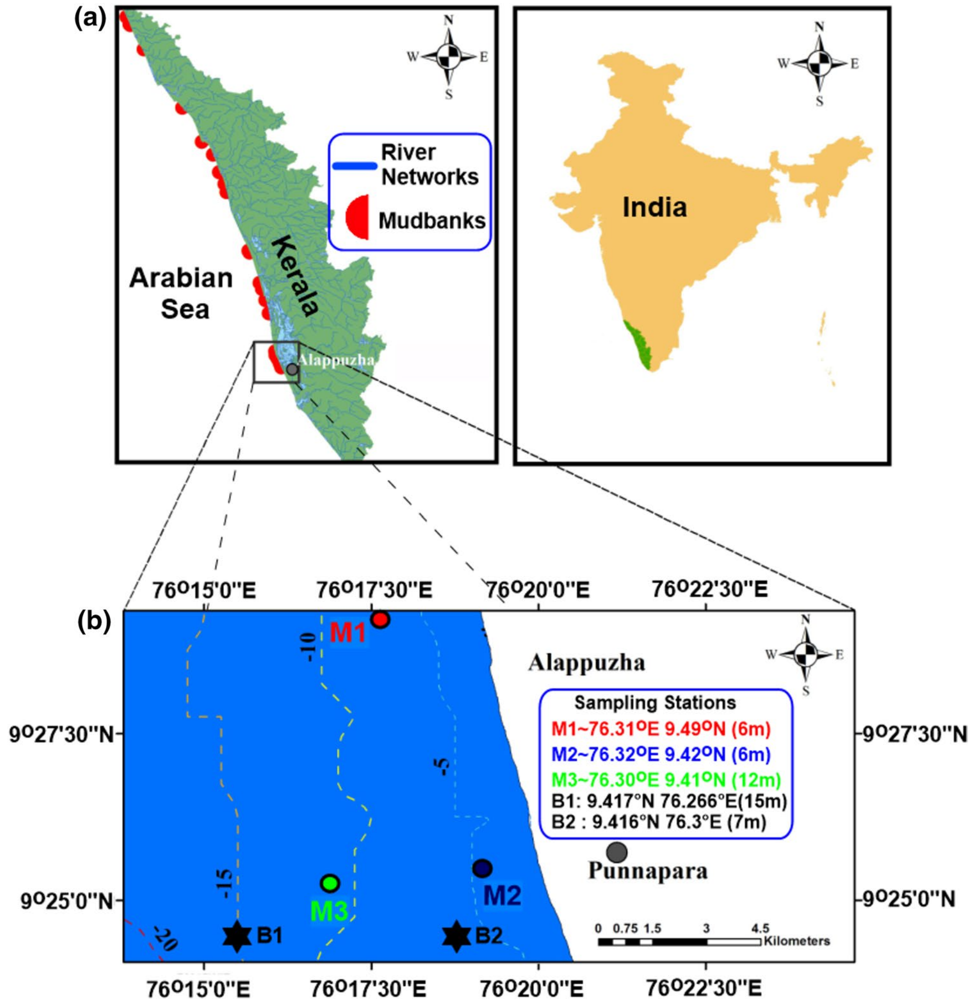

Fig. 1 **a** Map of showing the location of mudbanks along the Kerala, southwest coast of India. **b** Sediment (bedload, washload) sampling non-mudbank station marked by filled circle M1 (red) circle. The mudbank station are marked by M2 (blue) and offshore reference station marked by M3 (green). Wave rider stations (B1, B2) are marked by filled star (black). Present study area latitude and longitude values are given in legend (**b**) and water level given in brackets. (Modified from Gireeshkumar et al. (2017) copyright 2017, with permission from Elsevier)

southwest monsoon (June–September) and remaining in the northeast monsoon (October–December). A strong wind of about 30–60 km/h persists and changes its direction from south towards east during March–July. Littoral currents are stronger (~ 5–40 cm/s) during March–September and flows in south–southeast direction whereas cross shore currents become stronger towards north during November–January (Antony and Shenoi 1993; Narayana et al. 2001).

Materials and methods

Field sampling

As a part of "Alleppey Mudbank process studies (AMPS)", a joint field campaign was undertaken by CSIR-National Institute of Oceanography, Goa (CSIR-NIO) and Central Marine Fisheries Research Institute, Kochi (CMFRI). Three stations were selected for time series (April–August 2016) sediment sampling survey. Station M1 (6 m) represents a non-mudbank region, while M2 (6 m) is from a mudbank region which is approx ~ 7 km south of M1 (Fig. 1b). Station M3 is a reference site from the mudbank region and is located offshore to the west of station M2 at a depth of 12 m. Surface sediments (bedload) were collected using Van Veen grab and fluid (suspended load) samples using Niskin water sampler. The collected water was further filtered through 0.4-μm Millipore filter paper and the suspended fluid mud retained on the filter papers was later dried, weighed and packed for further analyses. In the laboratory, five representative samples collected on every sampling day from each station were selected and analysed for magnetic measurements. Hence, the one sample point in Figs. 2 and 7 represents the average value of five representative samples.

Environmental magnetic measurements

The dried (bedload, suspended) samples were weighed and packed in 8 cm^3 cylindrical plastic containers and the magnetic measurements were carried out at the paleomagnetic laboratory of CSIR-National Institute of Oceanography (NIO) in Dona Paula, Goa, India. Magnetic susceptibility

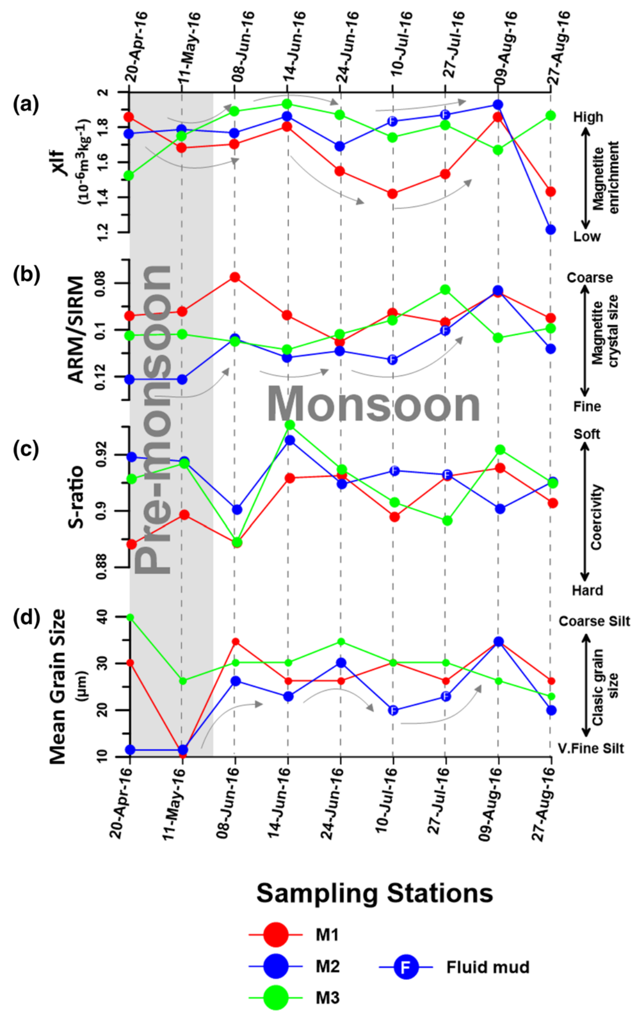

Fig. 2 Seasonal variations in **a** magnetic mineral concentration, **b** magnetic grain size, **c** magnetic mineralogy index (S-ratio) and **d** median grain size measured on surficial and fluid (suspended) mud samples from station are marked by solid lines, M1 (red), M2 (blue) and M3 (green). Please note that the scale of ARM/SIRM is reversed. Lower ARM/SIRM ratios indicate the dominance of coarser magnetic grain sizes and vice versa. The data of fluid mud samples has been marked as field circle with "F". The arrows are used only to highlight the trends in data sets

was measured at low frequency (0.47 kHz) using a Bartington MS2B meter. Anhysteretic remanent magnetization (ARM) was measured using AF-Demagnetizer with p-ARM attachment, 100 mT AF field was superimposed on a fixed DC bias field of 50 μT. Isothermal remanent magnetisation (IRM) of 1T in the forward direction and − 20, − 30 and − 300 mT in the backward direction were imparted using MMP10 pulse magnetizer and the remanence was measured using Molspin Minispin spinner magnetometer. Mass-normalized IRM acquired with a peak field of 1 T is assumed to be the saturation isothermal remanent magnetization (SIRM). *S*-ratio was calculated following the formulae, $S\text{-ratio} = IRM_{300mT}/IRM_{1T}$ (Thompson and Oldfield 1986; Bloemendal et al. 1988).

Specialized magnetic measurements were carried out at Environmental Magnetism Laboratory of Indian Institute of Geomagnetism (IIG), New Panvel, India. The hysteresis loop analyses were carried out on Princeton measurements of the micromag 2900 series alternating gradient magnetometer (AGM) in field cycling between + 1T. Temperature dependence of magnetic susceptibility was measured in a field of 300 A/m at 875 Hz by a CS3 furnace unit coupled to an Agico (KLY-4S) Kappabridge. The high-temperature measurements were performed from room temperature to 700 °C in argon atmosphere.

Grain size analysis

The grain size analyses of surface and fluid mud samples were carried out on Malvern Mastersizer 2000 Laser Particle Size Analyzer at CSIR- NIO in Dona Paula, Goa, India. For better dispersion, the samples were first desalinated and later dispersed by adding Na-hexametaphosphate and treated with ultrasonics. The organic carbon was removed using 10% H_2O_2 before the analysis. The values of grain size are reported in terms of volume %.

Magnetic mineral extraction and SEM-EDS analyses

Representative samples covering pre-monsoon and monsoon period were selected for extraction of magnetic particles from bulk sediment following the procedure of Petersen et al. 1986. Images of the magnetic particles were captured using a scanning electron microscope (JEOL JSM-5800 LV) in secondary electron (SE) imaging mode at energy levels between 15 and 20 kV. The elemental analysis was carried out using an energy-dispersive X-ray spectroscopy (EDS) probe attached to the microscope.

Hydrodynamics

Wave data were collected using two wave rider buoys to examine the influence of varying wave intensities on the mud dynamics during pre-monsoon and monsoon season. To cover scenarios of pre-mudbanks and mudbank formation stages, one wave rider buoy was deployed off Alappuzha coast at water depth of 15 m i.e., at location B1 and the wave data was collected for the duration between 21 May 2014 and 31 July 2014 (Fig. 1b). Soon after the formation of mudbank, an additional buoy was deployed at 7 m depth i.e., at location B2 on 26 June 2014, and wave data was gathered till 31 July 2014 (Fig. 1b). The locations B1 and B2 were at a distance of 10 km and 6 km from the shore. Wave data were recorded continuously for the duration of 10 min at the interval of 30 min.

The wave parameters and critical velocity required for entrainment of bedload sediments were calculated following Thornton and Guza 1983:

The sea bed orbital velocity (*u*) for pure wave motion was calculated using the following equation:

$$u = \frac{\pi H}{T}\frac{\cosh(k(h+z))}{\sinh(kh)} \quad (1)$$

where *H* is the wave height, *T* is the wave period, *h* is the water depth, *k* is the radian wave number and *z* is the elevation below still water level.

The critical velocities (u_{cr}) of different sediment grain sizes required to initiate the sediment movement from the seafloor was calculated using Komar and Miller 1973:

$$\frac{\rho {u_{cr}}^2}{(\rho_s - \rho)gD} = a''(d_o/D)^{1/2} \quad (2)$$

where ρ is the density of water, ρ_s is the sediment grain density, *g* is the acceleration due gravity, *D* is the sediment grain size, H_{rms} is the root mean square of wave height, $a''= 0.21$ is the proportionality coefficient calculated based on the average of Bagnold, 1946 and Manohar, 1955 and d_o is the sea bed orbital diameter given by:

$$d_o = \frac{H_{rms}}{\sinh(kh)} \quad (3)$$

Results

Magnetic and sedimentological characterization of surficial and suspended mud samples

Magnetic susceptibility (χ) and SIRM mainly reflects the magnetic mineral concentration, especially ferrimagnetic minerals such as magnetite (Thomson and Oldfield 1986). χ and ARM/SIRM values of bedload samples show variations in concentration and crystal size of magnetic particles (Fig. 2a, b). During pre-monsoon, the magnetic susceptibility at station M1 (non-mudbank) varies between 1.68 and 1.85×10^{-6} m^3 kg^{-1}. At station M2 and M3 (mudbank), χ varies from 1.52 to 1.78×10^{-6} m^3 kg^{-1} (Fig. 2a). During monsoon, we observed a trend of increase in magnetic susceptibility in samples from mudbank stations M2 and M3. The susceptibility values of bedload samples at stations M2 and M3 varies between 1.67 and 1.93×10^{-6} m^3 kg^{-1}, while the suspended samples of station M2 collected during monsoon (July 2016) period exhibits highest values of susceptibilities (1.83–1.87×10^{-6} m^3 kg^{-1}). It is interesting to note that, the susceptibility profile of M1 (non-mudbank) station showed a opposite trend of decrease in magnetic susceptibility compared to M2 and M3 (mudbank) station and the values range between 1.42 and 1.85×10^{-6} m^3 kg^{-1} (Fig. 2a).

The magneto-granulometric ratio, ARM/SIRM, is indicative of magnetic grain size, with higher values, suggesting fine grained i.e., single-domain (SD) and lower values for multidomain (MD) grains (Maher 1988; Thompson and Oldfield 1986). In the studied samples, ARM/SIRM ratio varies from 0.031 to 0.121 and higher values of χ is found to be dominated by coarser magnetic grains (Fig. 2b). A trend of coarsening in magnetic grain size is noticed with higher values of magnetic susceptibility are dominated by coarser magnetic grain sizes and are found to be concentrated during monsoon period at mudbank stations M2 and M3, while M1 shows a opposite trend (Fig. 2a, b). During pre-monsoon period, ARM/SIRM values are generally low in M1 compared to M2 and M3 and remains relatively stable but shows gradual decrease in χ at the onset of monsoon (Fig. 2a, b). Compared to station M1, we observed increase in values of magnetic susceptibility and linear decrease in ARM/SIRM ratio at stations M2 and M3 suggesting the dominance of coarser magnetic particles during monsoon period (Fig. 2a, b).

S-ratio is the measure of relative importance of low and high coercivity magnetic mineral components, with higher values corresponding to higher proportions of low-coercivity minerals (Thompson and Oldfield 1986; Bloemendal and Liu 2005). The S-ratio measured on all samples shows uniformity and values ranges between 0.88 and 0.93 regardless of sampling period (Fig. 2c). The majority of samples are characterized by high *S*-ratio (> 0.88) **indicating** that the magnetic mineralogy is dominated by low-coercivity minerals (Fig. 2c).

In studied samples, the physical grain size varies between 10.43 µm to 39.81 µm (Fig. 2d). A noticeable increase in mean grain size is observed with the commencement of monsoon indicating the period of increase in supply of coarse-grained clastic sediments in all three stations (Fig. 2d).

Grain size distribution of surface sediments

The seasonal variations in grain size distribution of samples representing pre-monsoon and monsoon from all three stations (M1, M2 and M3) are compared and presented in Fig. 3a–c. In general, the curves show a broad spectrum and well-sorted uni-modal distribution of sediment grain sizes covering very fine silt–coarse silt (Fig. 3a–c). Over all, the mean sediment grain size ranges from 10.43 µm to 39.81 µm (Fig. 2d). The sediments during pre-monsoon period are dominated by fine silt and grain size distribution curves gradually shift towards the medium-coarse silt during the monsoon period (Figs. 2d, 3a–c).

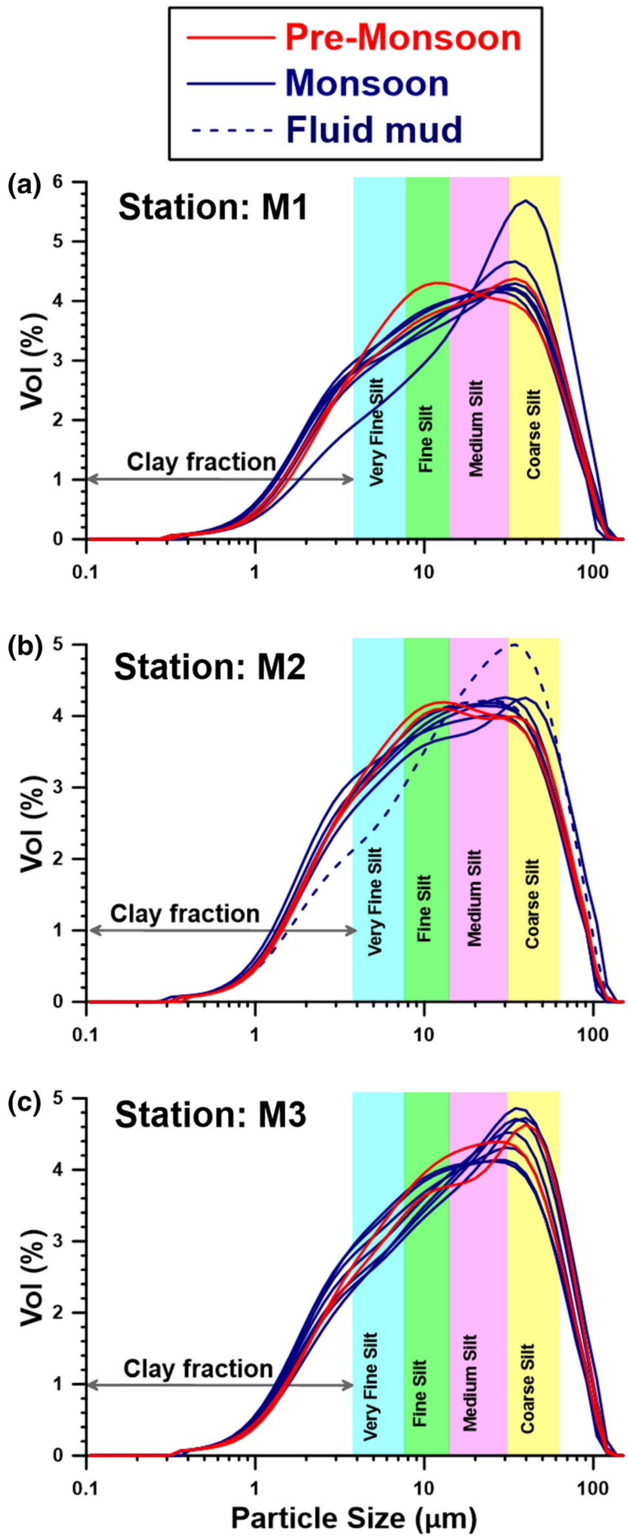

Fig. 3 Grain size distribution curves of surficial sediments (**a**–**c**), comparing the variations during pre-monsoon and monsoon period from stations M1, M2 and M3. The pre-monsoon curves are represented by solid red line and monsoon using solid blue line. The grain distribution curves of fluid mud samples of station M2 has been marked by solid dashed line in blue

Magnetic mineralogy and magnetic grain size from temperature-dependent magnetic susceptibility, hysteresis parameters and SEM-EDS analysis

The representative curves of temperature-dependent magnetic susceptibility for samples covering pre-monsoon and monsoon from all stations M1, M2 and M3 are shown in Fig. 4. A sharp decrease in magnetic susceptibility at high temperature i.e., above 550 °C suggests that the magnetic mineralogy is dominated by titano-magnetite (Fig. 4a–c). The χ-T curves show similarity to typical magnetite where all components gets removed between 550 and 600 °C (Fig. 4a–c) (Thompson and Oldfield 1986). The day plot shows that all the samples (regardless of sampling period) falls within the upper boundary of pseudo-single-domain (PSD) range (Fig. 5) (Day et al. 1977).

The electron microscopic images and EDS spectra of the magnetic grains extracted from the representative bulk surficial mud samples representing pre-monsoon and monsoon period in all three stations are presented in Fig. 6a–c. A large number of ferrimagnetic iron oxides of various sizes and shapes have been identified and they occur both as discrete as well as agglomerates (Fig. 6a–c). The EDS data of magnetic grains shows the presence of iron, titanium, oxygen with minor amounts of silicon, aluminium, magnesium, calcium, manganese and potassium (Fig. 6a–c).

Analysis of wave characteristics and transport dynamics of sediment grains at Alappuzha mudbanks

A maximum significant wave height (Hs) and peak wave period (T) were calculated in the nearshore waters of Alappuzha mudbank region. The maximum wave height of 3.16 m and 1.56 m and wave period of 6–20 s were observed at wave rider buoy stations (B1 and B2) (Samiksha et al. 2017). The seabed orbital velocities and critical velocities of sediment grains as calculated following Eqs. 1, 2 and 3 ("Hydrodynamics"). The criticial velocity (U_{cr}) calculated for all sediment grain sizes found at each station is calculated using Eqs. 2 and 3, the results are plotted in Fig. 7a. We observed that the critical velocities computed for all sediment grain sizes at station M1, M2 and M3 are higher during monsoon periods and mimics the sea bed orbital velocity profiles (data not shown) (Fig. 7a–c). These observations suggest that the higher wave and bottom current conditions required for initiation of sediment bed movement (entrainment and suspension) are available only during the monsoon period.

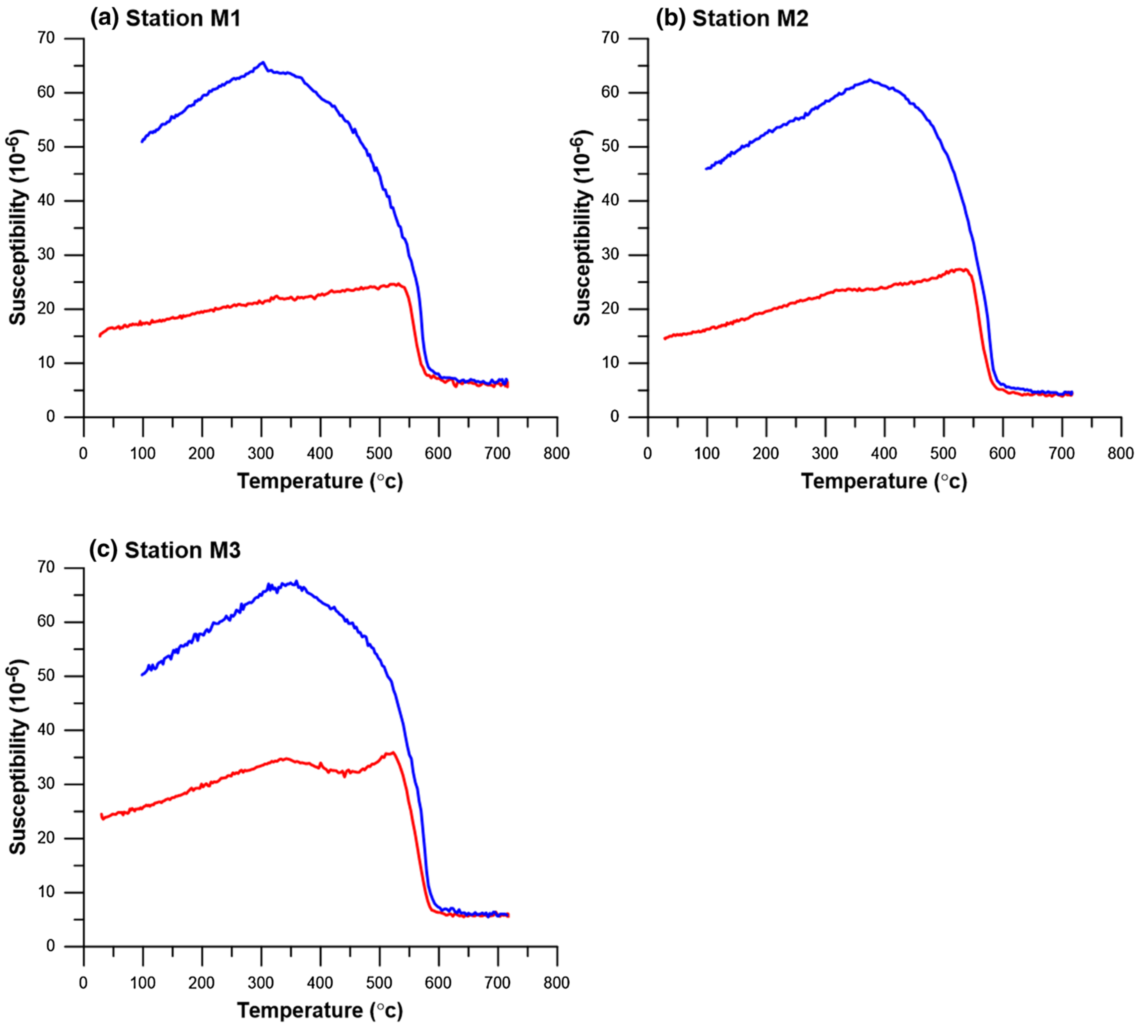

Fig. 4 Temperature dependence magnetic susceptibility curves of the representative (monsoon period) samples from stations **a** M1, **b** M2 and **c** M3. A solid red line indicates heating curve and blue line indicates cooling curve

Relationship between environmental magnetic and sedimentological parameters of bedload and suspended load samples

Bivariate plots were used to examine the relationship between magnetic and sedimentological parameters (Fig. 8a–d). A good covariation between χ and SIRM suggest that the majority of the sediments are dominated by ferrimagnetic minerals since para and diamagnetic minerals has very less influence SIRM values (Thompson and Oldfield 1986) (Fig. 8a). We noticed some minor differences in χ and SIRM values. The grain-size independent parameter (χ) possessed higher values and exhibits large scattering, while dependent parameter (SIRM) showed narrow scattering (vertical and horizontal) and possesses much lower values (Fig. 8a).

Coupling between magnetic grain size and magnetic susceptibility is generally weak in all samples (Fig. 8b). At mudbank stations (M2 and M3), the large variations in ARM/SIRM and narrow range in χ suggest that bulk magnetic signal is carried by both fine as well as coarse size magnetic grains (Fig. 8b). The samples from non-mudbank station (M1) exhibits opposite trend with samples showed relatively narrow range in magnetic grain size and much broader range in χ (Fig. 8b). A strong relationship exists between magnetic grain size and physical grain size for all samples implying that the magnetic particle size and clastic sediment grain size are largely adjunct (Fig. 8c). The coupling between χ and physical grain size is weak for all samples (Fig. 8d). The magnetite concentrations are quite variable and contained in two dominant fractions (10.43–11.48 μm and 19.95–39.81 μm) (Fig. 8d).

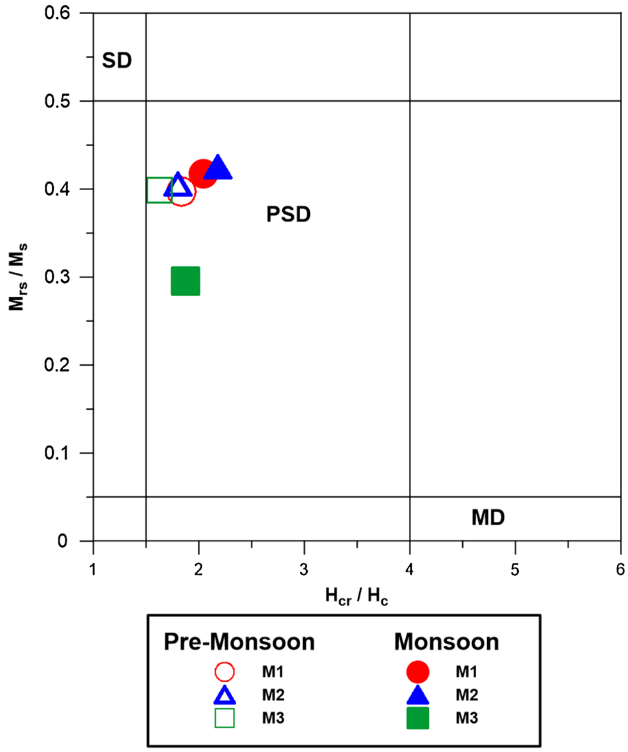

Fig. 5 Hysteresis parameters of samples from M1, M2 and M3 stations are incorporated in a Day plot (Day et al. 1977). Open symbols indicate samples from pre-monsoon period and closed symbols indicate samples from the monsoon period

Discussion

In this section, we discuss our data-based observations (environmental magnetism, sedimentology and hydrodynamics) to examine the linkages between enrichment of silt-size magnetic particles and underlying responsible physical and sedimentary processes (entrainment, transport, sorting, settling and enrichment) associated with the formation of mudbanks along Alappuzha Coast.

Magnetic and sedimentological signatures of entrainment, fractionation and transport of magnetic particles

In coastal systems, the mixing, fractionation, transport and enrichment of magnetic particles is controlled by the complex interaction between sedimentary processes, sediment composition and prevailing hydrodynamic conditions (Rao 1957; Slingerland 1977; Komar and Wang 1984; Frihy and Dewidar 2003; Gallaway et al. 2012). In order to investigate the formation processes of mudbanks, we carefully examined the linkages between sediment magnetic signature and grain size characteristics of surficial and suspended sediment load from one non-mudbank station (M1) and two mudbank stations (M2, M3) located off southwest coast of India.

In calmer conditions, especially during pre-monsoon period, majority of the clastic as well as magnetic particles remains as a bedload owing to relatively weaker

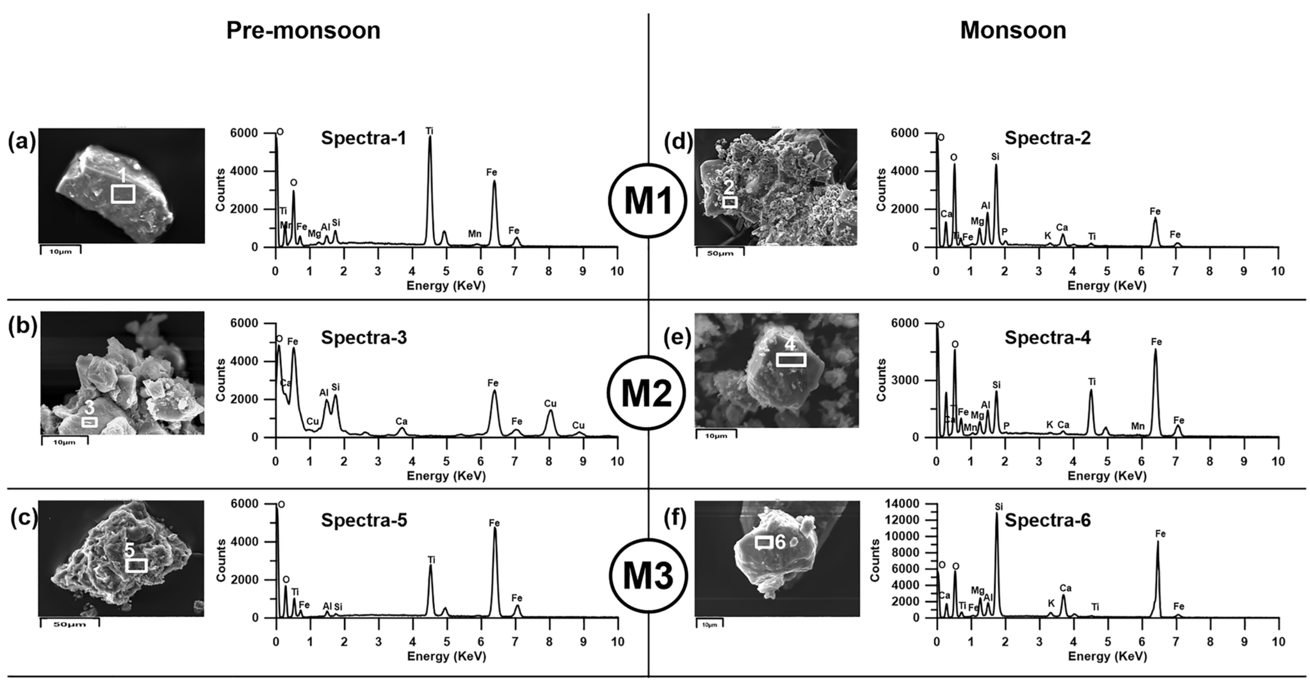

Fig. 6 SEM images and EDS spectra of magnetic particles extracted from representative surface sediment samples covering pre-monsoon and monsoon season from stations: M1(**a, d**), M2 (**b, e**) and M3 (**c, f**)

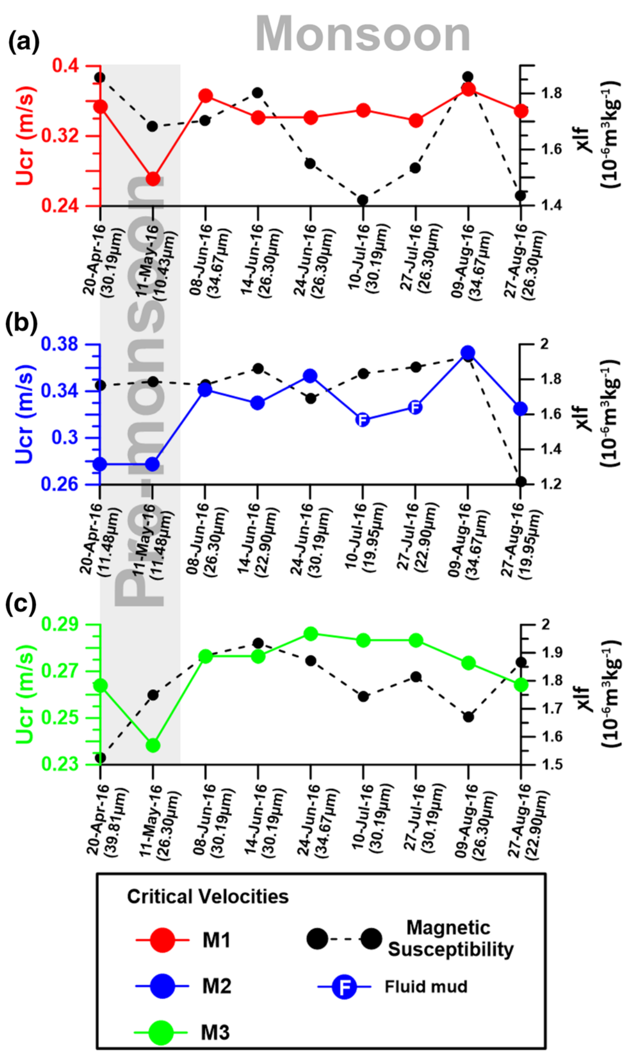

Fig. 7 Calculated critical velocities for representative sediment grain sizes covering pre-monsoon and monsoon period for stations **a** M1(red), **b** M2 (blue) and **c** M3 (green) marked by solid lines and the corresponding scale is in the left. The magnetic susceptibility of the same samples is plotted at the right side and is marked by dash lines (black). Sample collection date and mean grain size are shown

hydrodynamics which facilitates poor sorting resulting in the formation of mixed grain size (clastic) and magnetically low-enriched sediment bed (as seen from magnetic susceptibility data, Fig. 2a). In the studied samples, less variability in concentration and grain size of magnetic minerals, presence of mixed (fine and coarse silt)-sized clastic grains and availability of lower critical velocities required for entrainment at all three stations during pre-monsoon period suggest that the calm and weaker hydrodynamics allowed retention of both fine and coarse silt-sized magnetic and non-magnetic fractions on seafloor (Figs. 2a, b, d, 7a–c). This further implies that the enrichment of magnetic particles by selective entrainment is not favored during the pre-monsoon period.

At the onset of monsoon, when the wave and current velocities are higher the sediments are more easily entrained, sorted and transported to distal regions depending on the energies of the incoming waves and bottom currents. As a result, the denser and finer magnetic fraction within the bulk mud-rich sediment settles quickly on sea bed and get buried, while lighter clastic fraction gets easily entrained and remains in suspension for longer period. An increase in ferrimagnetic mineral concentration and coarsening in magnetic grain sizes is observed as reflected by higher χ and lower ARM/SIRM values at mudbank stations (M2 and M3) is noticed (Fig. 2a, b). This can be explained by the fact that, higher bottom velocities during monsoon facilitate intense churning, mixing and suspension of bottom mud-rich sediments which later gets fractionated according to their hydraulic equivalences. Further, the gravitational sorting in combination with selective entrainment causes quick settling of coarser magnetic fraction from the bulk mud-rich sediments while finer non-magnetic fraction either remains in suspension as long as higher energies persists or gets transported alongshore or crosshore depending upon the energies of the littoral current system.

The availability of sufficient critical velocities to entrain the sediment grain sizes at all three (M1, M2, M3) stations during monsoon period indicates that entire bottom sediments are churned up and brought into suspension and simultaneously coarser silt-size magnetic fraction settles on the bed while finer silt-size magnetic fractions remains as suspended load (Fig. 7a–c). It is highly possible that the continuous suspension of the bottom sediments throughout the monsoon period result in accumulation of finer silt-size magnetic particles in the water column forming thick fluid mud and consequently forms mudbanks. It is interesting to note that the fluid mud samples collected during monsoon (10 July 2016 and 27 July 2016) at station M2 showed highest values of χ and relatively lower mean grain size (19.95–22.90 µm) (Fig. 2a, b and d; Fig. 7b). This observation supports the above hypothesis.

Controls of sediment provenance, seafloor morphology, and grain size on mudbank formation

In addition to wave and current climate, the formation of mudbanks is also influenced by the bathymetry, provenance and supply of mud. In this section, we discuss the significance of all these factors controlling the formation of mudbanks along Alappuzha coast. The mudbanks formed along Alappuzha coast are unique as there is no major river systems supplying the mud-rich sediments to the coast and nearshore areas (Kurup 1972). Several hypotheses were proposed to explain the potential sources of the mud to the Alappuzha Coast. Gopinathan and Qasim (1974) suggested that mud from offshore region (greater > 20 m) are brought

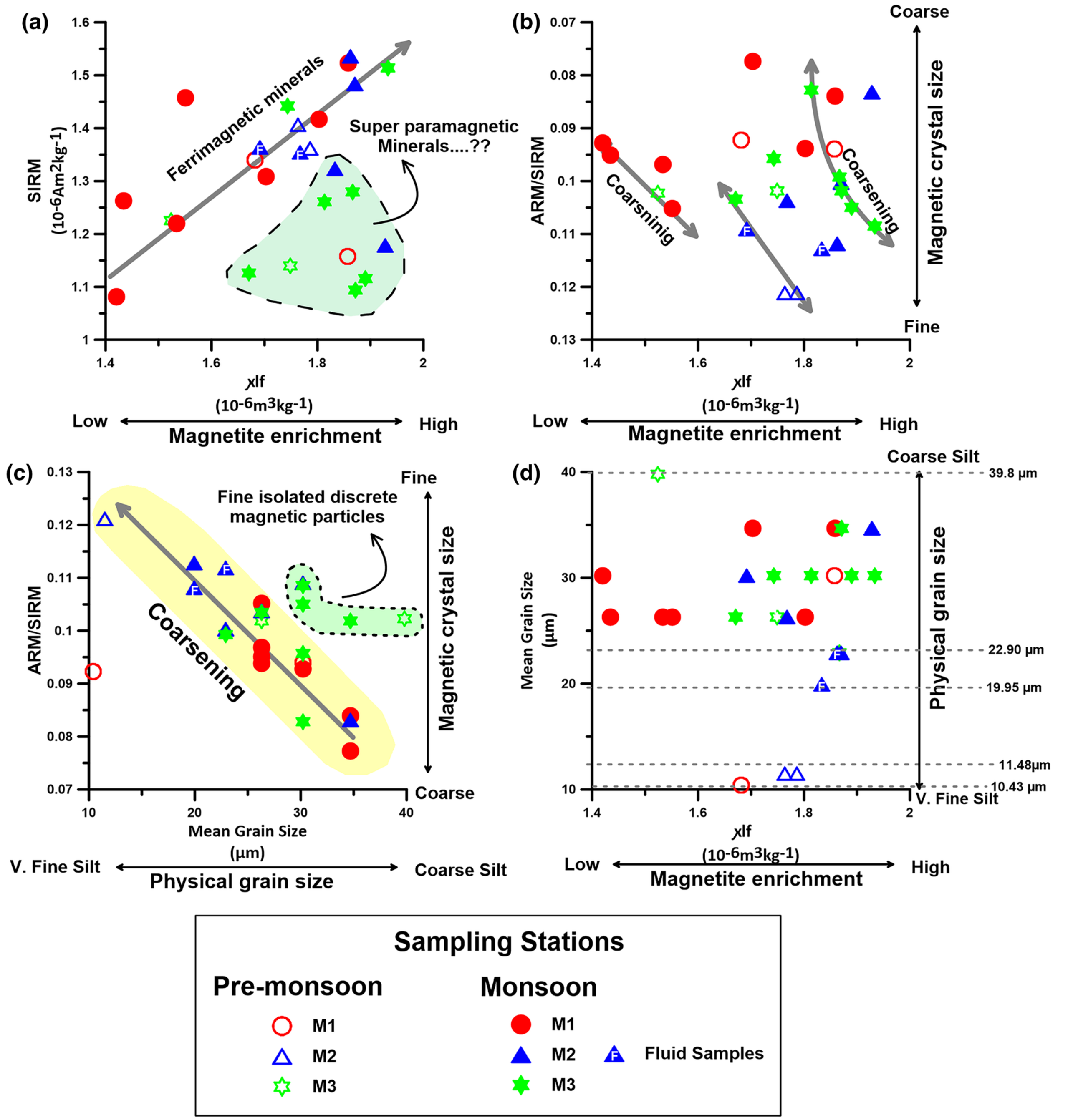

Fig. 8 Scatterplots (**a**–**d**) comparing magnetic parameters and clastic grain sizes of surface and fluid (suspended) mud samples from Alappuzha non-mudbank (M1) and mudbank region (M2, M3). Open symbols indicate samples from pre-monsoon period and closed symbols indicate samples from the monsoon period

to the nearshore areas by strong currents during southwest monsoon. Recent study by Muraleedharan et al. 2017 reported that Alappuzha region receives the fluid mud from the offshore depocenter in the shelf which gets transported to the coast through depression channel network. Presence of buried paleo-channels, cracks, mud cones (coastal zone) and lime shell beds in deeper strata of proximal Vembanad lagoon (terrestrial zone) of Alappuzha region structures acts as a potential conduits for the transport of mud from terrestrial sources to the coast and nearshore regions of Alappuzha (King 1881; Crawford 1860 in Bristow 1938 (cross ref.); Nair 1976; Gopinathan et al. 1983; Balachandran 2004; Loveson et al. 2016). The source of the fluid mud to this region still remains an ambiguity (Kurup 1972).

Magnetic data showed variations in distribution of magnetic minerals and highest concentrations were found in M2 and M3 compared to relatively lower at M1 station. Next question to be answered was why the samples at M1 (non-mudbank) station showed lower enrichment of magnetic particles even when the sufficient critical velocities required for entrainment of mud are available at both M1 and M2 stations (Figs. 2a, 7a). The environmental magnetic data of surficial and suspended mud showed highest magnetic concentrations at mudbank stations (M2, M3) and relatively low at non-mudbank (M1) station, while magnetic mineralogy and magnetic grain size remains unchanged as confirmed by room temperature, temperature-dependent magnetic measurements and SEM-EDS analysis (Figs. 2b, 4a–c, 6). This finding confirms that sediment provenance is not the critical factor governing the formation of mudbanks along Alappuzha coast. It is interesting to note that the distance between station M1 and M2 is ~7 km and if these geological structures were the potential conduits for the transport of fluid mud from terrestrial sources to nourish the Alappuzha coast, then one would expect the similar magnetite concentrations at stations M1 and M2 as well (Fig. 2a). Therefore, we hypothesize that the observed differences in the distribution of ferrimagnetic mineral concentrations between M1 and M2 is due to the different partitioning regime controlled by prevailing littoral drift system and changing conditions of bottom currents. The dilution by magnetite-deficient mud could be another factor causing variations in magnetic susceptibility between M1 M2, and M3 stations (Thompson and Oldfield 1986). As there is no major feeder of mud to the Alappuzha coast, the possibility of dilution of magnetic signal from other sources can be ruled out.

Changes in the sea floor morphology can significantly control the sediment dynamics. As observed from the sea floor bathymetric data, there are no significant changes on the morphology of the sea floor at all three stations (Fig. 1b). Hence it is unlikely that sea floor morphology had any significant influence over the formation of mudbanks along Alappuzha coast. More detailed high-resolution close-grid bathymetric mapping of this area would help to delineate the mud distribution pattern.

In fluvial, coastal and marine environments, the sediment grain size responds differently to varying hydrodynamic conditions as it influences grain-size selective as well as mineral-density-based selective sorting during the course of sediment transport and deposition and controls the overall sediment distribution (Slingerland 1977; Komar and Wang 1984; Gallaway et al. 2012; Badesab et al. 2017). During calmer conditions, especially in low-energy-dominated rivers and creeks, uni-directional flow velocity constrains sediment fractionation process resulting in accumulation of mixed (interms of grain sizes) and poorly sorted sediment bed. In estuarine and nearshore coastal environments, higher bottom currents generated by tidal and wave actions initiate sediment bed movement and allows better sediment mixing and sorting. During this process, lighter, especially, silicate minerals are entrained first and gets easily transported to the distal areas, while the denser (fine-coarse) magnetic fraction will quickly settle on the sea bed forming enriched bed (Slingerland, 1977). In the studied samples, the grain size distribution of surface (bedload) and fluid (suspended) samples from Alappuzha exhibits spatial variability during pre-monsoon and monsoon season (Fig. 3a–c). The dominance of fine-medium silt-size clastic grains in all three stations during pre-monsoon is suggestive of poor mud partitioning regime due to weaker hydrodynamic which favors grain size-selective sorting (Fig. 3a–c). Recently, Muraleedharan et al. 2017 reported that during southwest monsoon period, the wind and wave energies are significantly higher which cause intense churning of bottom sediments thereby creating suspension of fine particles leading to the formation of fluid mud at Alappuzha. A trend of increase in physical grain size, critical velocities, coarsening in magnetic grains (as indicated by lower ARM/SIRM) and higher χ suggests that higher current velocities generated during southwest monsoon cause continuous disturbance and churning of bottom sediments resulting in intense suspension and better sorting and thereby favors mineral density-based selective sorting (Figs. 2a, b, d, 7a–c). As a result, the finer magnetic fraction (washload) either remains in suspension forming thick fluid mud or gets transported alongshore. The highest values of χ and occurence of finer physical grain sizes (19.95 µm, 22.90 µm) in the suspended load of fluid mud at station M2 during monsoon period supports the above interpretation (Fig. 2a, d). As compared to fluid mud (suspended), denser and coarse magnetic (bedload) fraction is less entrained and even after initial churning they quickly settle on the sea bed forming magnetite-rich zone during monsoon period. The higher susceptibility and dominance of medium-coarse silt-size clastic grains at station M2 and M3 provide evidences to the above interpretation (Fig. 2a, d).

Linkages between magnetic enhancement and mudbank formations

It is interesting to note that with the commencement of monsoon, magnetic susceptibility profile of non-mudbank station (M1) exhibit opposite trend showing decrease in magnetite concentration compared to magnetically enriched mudbank stations (M2, M3) (Fig. 2a). Next question to be answered was whether there are any linkage between magnetic enhancement/depletion and formation of fluid mud. The highest values of χ and occurrences of finer physical grain sizes (19.95 µm, 22.90 µm) in fluid mud samples at mudbank station M2 during monsoon suggest that the magnetic particles are also found to be concentrated in fine-medium silt-size fraction of fluid mud (Fig. 2a, d). We hypothesize that the observed decrease in magnetite concentrations at non-mudbank station M1 during monsoon period is mainly due to significant loss of magnetically rich fine (suspended) and medium-coarse (bedload) silt-sized grains caused as a result of rapid sediment transport driven by strong littoral alongshore currents. Past work by several researchers has demonstrated that the lateral movement of fluid mud is controlled by littoral currents along Kerala Coast (Varma and Kurup 1969; Kurup 1977; Mallik et al. 1988) and this observation supports the above interpretation. The above observations also hint on the need for carrying out high-resolution time series and precise sampling for magnetic mapping of magnetite-rich bedload and suspended load covering nearshore and offshore regions off Alappuzha. This would further help to delineate the mud depocenter (magnetically enriched) and further increase our understanding on the sediment fractionation processes responsible for mudbank formation.

Influence of particle-size variations and sediment diagenesis on the magnetic properties

In coastal and nearshore environments, variability in hydro-sediment dynamics can result in particle-size sorting during the course of sediment transport and deposition (Oldfield and Yu 1994; Gallaway et al. 2012; Badesab et al. 2012; Rahman and Plater 2014). The dependence of magnetic properties on bulk sediment grain size has been successfully used to infer the hydrodynamic variations in estuarine and coastal environments (Hatfield et al. 2010; Gallaway et al. 2012; Badesab et al. 2012, 2017). A strong relationship exists between magnetic grain size and physical grain size for majority of the samples suggests that the magnetic and clastic grain size are dependent (Fig. 8c). In all three stations, the decrease in physical grain size, relatively stable χ and magnetic grain size during pre-monsoon suggests that in calmer coastal sedimentary systems, ferrimagnetic minerals are insensitive to hydrodynamic sorting (Fig. 2a, b, d) (Nguyen et al. 2016).

The post-depositional processes including sediment diagenesis and authigenesis can alter the magnetic mineral assemblages (Karlin and Levi 1985; Snowball 1993; Dewangan et al. 2013; Roberts 2015; Badesab et al. 2017). Our study area lies in highly dynamic coastal environment where the sediments gets regularly suspended and flushed to sea by changing hydrodynamics. In the studied surface samples, dominant magnetic mineralogy is possessed by fine-coarse silt-size magnetic (Fe-Ti rich) particles as confirmed by room temperature and temp-dependent magnetic measurements (Figs. 2a, b, 4a–c, 5). In addition, we did not observe presence of any secondary diagenetic minerals such as iron sulfides in our SEM-EDS data as compared with strongly reducing conditions which is often observed in shelf and deep-sea sediment cores (Roberts and Turner 1993; Roberts 1995; Maher and Thompson 1999; Dewangan et al. 2013; Badesab et al. 2017). Therefore, it is highly unlikely that sediment diagenesis has any major influence on magnetic properties of surficial and fluid samples from Alappuzha region.

Conclusion

In this study, we examined the linkages between sediment magnetic signatures and mudbank formative mechanism. We document the relation between enrichment of magnetite and mudbank formation (Fig. 8b). This could be used as an important fingerprint for identifying the potential sites of mudbanks. However, this linkage needs to be further exploited in other mudbank-forming environments and establish it as a potential proxy for identifying the sites of mudbanks in coastal and shelf sedimentary system.

We relate our data-based observations (environmental magnetism, sedimentology and hydrodynamics) to magnetically track the physical and sedimentary processes (entrainment, transport, sorting, settling, and enrichment of mud) associated with the formation of mudbanks.

Based on the sediment magnetic (enrichment and depletion) and sedimentological signatures, we have developed a conceptual model, which explains the formative mechanism of mudbanks along Alappuzha Coast (Fig. 9). This model can be very well applied to investigate sediment dynamics in other mud-rich coastal and shelf sedimentary systems.

High-resolution sea floor mapping, time series sampling (weekly) and precise magnetic and sedimentological analysis of bedload and fluid mud samples from mudbank and non-mudbank regions is required to delineate the sedimentary structures of magnetite-rich zones for better understanding of physical processes associated with mudbank formation in coastal systems.

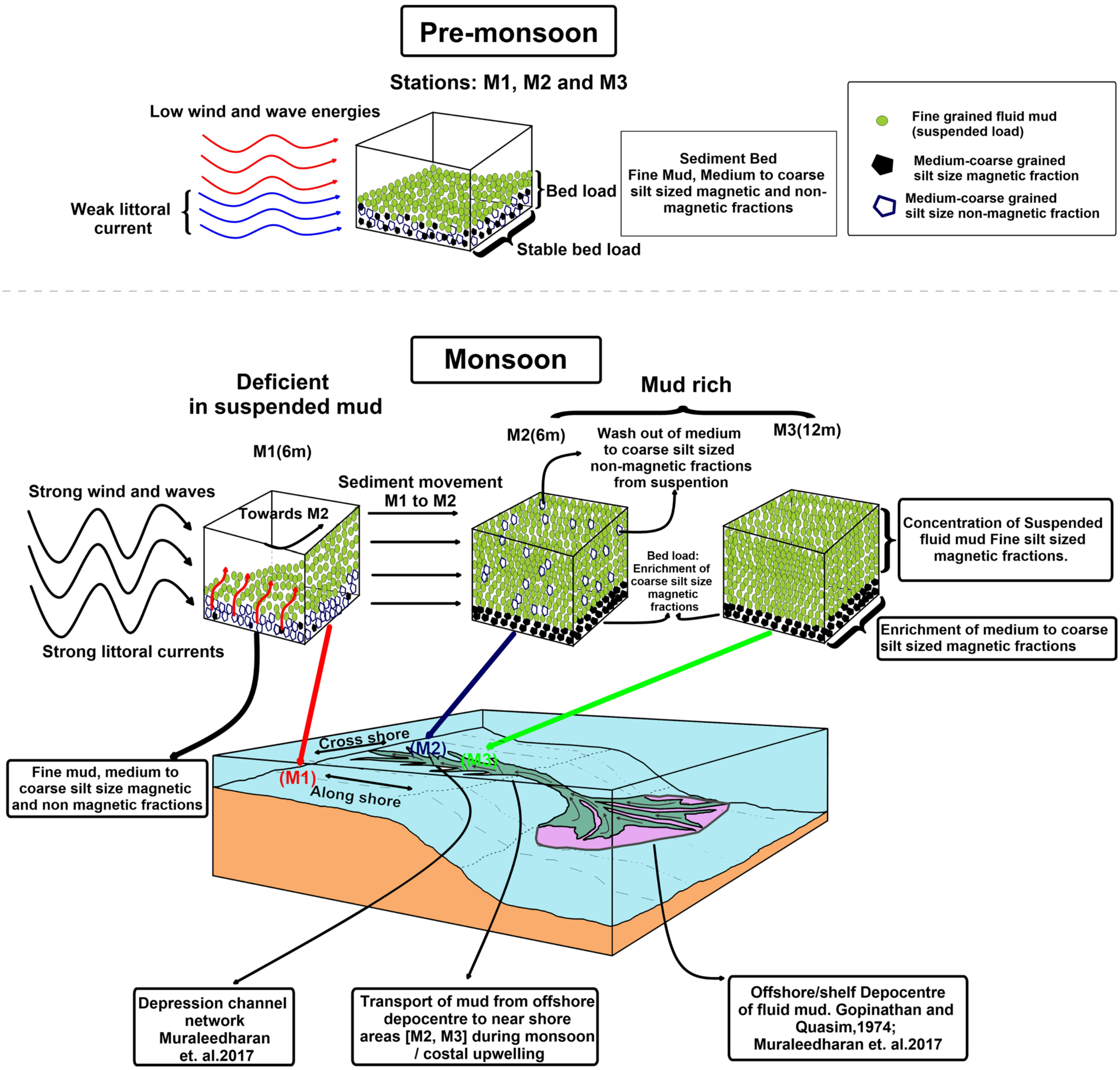

Fig. 9 Conceptual model explaining the sediment dynamics associated with the formation of mudbank off Alappuzha in Kerala state, southwest coast of India

Acknowledgements The present work forms part of the Alappuzha Mudbank Process Studies (AMPS), a joint program between CSIR–National Institute of Oceanography (CSIR–NIO), Goa, its Regional Centre (RC) at Kochi, and Central Marine Fisheries Research Institute (CMFRI), Kochi. We thank Director, CSIR-NIO, Goa for providing facilities to carry out this work. Our special thanks to Dr. S.W.A. Naqvi, former Director, CSIR-NIO for his support and keen interest in this study. We also thank Dr. A. Gopalakrishnan, Director, CMFRI, for his active involvement in this program and providing FV Silver Pompano for data collection. The authors thank Dr. N. Ramaiah, Chairman, Mentor Group for CSIR–NIO RC–Kochi, for his contribution to AMPS. We acknowledge the Indian National Centre for Ocean Information Services (INCOIS), MoES, for providing wave data at Kollam. We are also thankful to Sudheesh, Lakshmikant and Ravish for their help during field work. The CSIR-NIO contribution number is 6284.

References

Allison MA, Lee MT (2004) Sediment exchange between Amazon mudbanks and shore-fringing mangroves in French Guiana. Mar Geol 208:169–190

Allison MA, Lee MT, Ogston AS, Aller RC (2000) Origin of Amazon mudbanks along the northeastern coast of South America. Mar Geol 163:241

Anthony EJ, Orford JD (2002) Between wave- and tide-dominated coasts: the middle ground revisited. J Coast Res Spec Issue 36:8–15

Anthony EJ, Dolique F, Gardel A, Gratiot N, Polidori L, Proisy C (2007) Near shore intertidal topography and topographic-forcing mechanisms of an Amazon-derived mudbank in French Guiana. Cont Shelf Res 28(6), 813–822

Anthony EJ, Franck D, Antoine G, Nicolas G, Christophe P, Laurent P (2008) Nearshore intertidal topography and topographic-forcing mechanisms of an Amazon-derived mud bank in French Guiana. Cont Shelf Res 28(6):813–822. https://doi.org/10.1016/j.csr.2008.01.00 **(ISSN 0278–4343)**

Anthony EJ, Antoine G, Nicolas G, Nicolas G, Mead A, Franck D, François FR (2010) The Amazon-influenced muddy coast of South America: a review of mud-bank–shoreline interactions. https://doi.org/10.1016/j.earscirev.2010.09.008

Antony MK, Shenoi SSC (1993) On the flow, thermal field and winds along the western continental shelf of India. Cont Shelf Res 13(4):425–439. https://doi.org/10.1016/0278-4343(93)90059-7 **(ISSN 0278–4343)**

Badesab F, vonDobeneck T, Bryan KR, Müller H, Briggs RM, Frederichs T, Kwoll E (2012) Formation of magnetite-enriched zones in and offshore of a mesotidal estuarine lagoon: an environmental magnetic study of Tauranga Harbour and Bay of Plenty, New Zealand. Geochem Geophys Geosyst 13:Q06012. https://doi.org/10.1029/2012GC004125

Badesab F, von Dobeneck T, Briggs RM, Bryan KR, Just J, Müller H (2017) Sediment dynamics of an artificially deepened mesotidal coastal lagoon: an environmental magnetic investigation of Tauranga Harbour, New Zealand. Estuar Coast Shelf Sci 194:240–251. https://doi.org/10.1016/j.ecss.2017.06.017

Balachandran KK (2004) Does subterranean flow initiate mud banks off the southwest coast of India? Estuar Coast Shelf Sci 59(4):589–598. https://doi.org/10.1016/j.ecss.2003.11.004 **(ISSN 0272–7714)**

Bloemendal J, Xiuming L (2005) Rock magnetism and geochemistry of two plio–pleistocene Chinese loess–palaeosol sequences—implications for quantitative palaeoprecipitation reconstruction. Palaeogeogr, Palaeoclim, Palaeoecol 226(1–2):149–166. https://doi.org/10.1016/j.palaeo.2005.05.008 **(ISSN 0031–0182)**

Bloemendal J, Lamb B, King J (1988) Paleoenvironmental implications of rock-magnetic properties of late quaternary sediment cores from the eastern equatorial Atlantic. Paleoceanography 3(1):61–87. https://doi.org/10.1029/PA003i001p00061

Borreswara Rao C (1957) Beach erosion and concentration of heavy mineral sands. J Sediment Petrol 27(2):143–147

Bristow RC (1938) Cochin harbour development: history of mud banks 1. Cochin Govt. Press, Ernakulam, pp 174

Cioppa MT, Porter NJ, Trenhaile AS, Igokwe B, Vickers J (2010) Beach sediment magnetism and sources: Lake Erie, Ontario, Canada. J Great Lakes Res 36(4):674–685. https://doi.org/10.1016/j.jglr.2010.07.007

Crawford JWC (1860) History of mud banks. Cochin Goverment Press, Cochin

Damodaran R, Hridayanathan C (1966) Studies on the mud banks of the Kerala coast. Bull Dept Mar Biol Oceanogr Univ Kerala 2:61–68

Day R, Fuller M, Schmidt VA (1977) Hysteresis properties of titanomagnetites: grain-size and compositional dependence. Phys Earth Planet Inter 13(4):260–267. https://doi.org/10.1016/0031-9201(77)90108-X **(ISSN 0031–9201)**

Dewangan P, Basavaiah N, Badesab FK, Usapkar A, Mazumdar A, Joshi R, Ramprasad T (2013) Diagenesis of magnetic minerals in a gas hydrate/cold seep environment off the Krishna–Godavari basin, Bay of Bengal. Marine Geol 340:57–70. https://doi.org/10.1016/j.margeo.2013.04.016 **(ISSN 0025–3227)**

Eisma D, Van der Marel HW (1971) Marine muds along the Guyana coast and their origin from the Amazon basin Contr. Miner Petrol 31:321. https://doi.org/10.1007/BF00371152

Eric G, Alan ST, Maria TC, Robert GH (2012) Magnetic mineral transport and sorting in the swash-zone: northern Lake Erie. Canada Sedimentol 59:1718–1734. https://doi.org/10.1111/j.1365-3091.2012.01323.x

Evans ME, Heller F (2003) Environmental magnetism: principles and applications of enviromagnetics. Academic Press, San Diego, pp 299. https://doi.org/10.1002/jqs.858

Foster IDL, Albon AJ, Bardell KM, Fletcher JL, Jardine TC, Mothers RJ, Pritchard MA, Turner SE (1991) High energy coastal sedimentary deposits—an evaluation of depositional processes in Southwest England. Earth Surf Process Landf 16:341–356. https://doi.org/10.1002/esp.3290160407

Frihy OE, Dewidar KM (2003) Patterns of erosion/sedimentation, heavy mineral concentration and grain size to interpret boundaries of littoral sub cells of the Nile delta, Egypt. Mar Geol 199:27–43. https://doi.org/10.1016/S0025-3227(03)00145-2

Froidefond JM, Pujos M, Andre X (1988) Migration of mudbanks and changing coastline in French Guiana. Mar Geol 84:19e30. https://doi.org/10.1016/j.ecss.2015.07.018

Gallaway E, Trenhaile AS, Cioppa MT, Hatfield RG (2012) Magnetic mineral transport and sorting in the swash-zone: northern Lake Erie. Can Sedimentol 59:1718–1734. https://doi.org/10.1016/j.margeo.2016.11.014

Gireeshkumar TR, Mathew D, Pratihary AK, Naik H, Narvekar KU, Araujo J, Balachandran KK, Muraleedharan KR, Thorat B, Nair M, Naqvi SWA (2017) Influence of upwelling induced in near shore hypoxia on the Alappuzha mud banks, South west coast of India. Contshelf Res 139:1–8. https://doi.org/10.1016/j.csr.2017.03.009

Gopinathan CK, Qasim SZ (1974) Mud banks of Kerala—their formation and characteristics. Indian J Mar Sci 3(2):105–114. http://nopr.niscair.res.in/handle/123456789/39561

Gopinathan CK, Raghunathan A, Rao DS, Mathew KJ, Murty AVS (1983) Source of mud of Alleppey mud bank mud core and the message it conveys. Bull Cent Mar Fish Res Inst 31:18–20

Hatfield RG, Maher BA (2008) Suspended sediment characterization and tracing using a magnetic fingerprinting technique: Bassenthwaite Lake, Cumbria, UK. Holocene 18(1):105–115. https://doi.org/10.1177/0959683607085600

Hatfield RG, Cioppa MT, Trenhaile AS (2010) Sediment sorting and beach erosion along a coastal foreland: magnetic measurements in Point Pelee National Park, Ontario, Canada, Sediment. Geol 231:63–73. https://doi.org/10.1016/j.sedgeo.2010.09.007

Jacob PG, Qasim SZ (1974) Mud of a mud bank in Kerala, south–west coast of India. Indian J Mar Sci 3:115–119. http://eprints.cmfri.org.in/id/eprint/7310

Jacob N, Ansari MA, Revichandran C (2015) Environmental isotopes to test hypotheses for fluid mud (mud bank) generation mechanisms along the southwest coast of India Estuarine. Coast Shelf Sci 164:115–123. http://drs.nio.org/drs/handle/2264/4883

Karlin R, Levi S (1985) Geochemical and sedimentological control of the magnetic properties of hemipelagic sediments. J Geophys Res 90(B12):10373–10392. https://doi.org/10.1029/JB090iB12p10373

Karnan C, Jyothibabu R, Arunpandi N, Jagadeesan L, Muraleedharan KR, Pratihari AK, Balachandran KK, Naqvi SWA (2017) Discriminating the biophysical impacts of coastal upwelling and mud banks along the southwest coast of India. J Mar Syst 172:24–42. https://doi.org/10.1016/j.jmarsys.2017.02.012 **(ISSN 0924–7963)**

King W (1881) Mudbanks of Narakkal and Alleppey on the Travancore coast. Record of Geological Survey of India, 17

Komar PD, Miller MC (1973) The threshold of sediment movement under oscillatory water waves. J Sediment Res 43(4)

Komar PD, Wang C (1984) Processes of selective grain transport and the formation of placers on beaches. J Geol 92:637–655. https://doi.org/10.1086/628903

Krishnan MS (1968) The evolution of the coasts of India. Bull Nat Sci Acad 38:398–404

Kurup PG (1972) Littoral currents in relation to the mud bank formation along the coast of Kerala. Mahasagar 5(3):158

Kurup PG (1977) Studies on the physical aspects of the mudbanks along the Kerala coast with special reference to the Purakad mud bank (PhD thesis). University of Cochin, Cochin, Kerala, India

Liu JP, Li AC, Xu KH, Velozzi DM, Yang ZS, Milliman JD, DeMaster DJ (2006) Sedimentary features of the Yangtze River-derived along-shelf clinoform deposit in the East China Sea. Cont Shelf Res 26:2141–2156

Loveson VJ, Dubey R, Kumar DR, NigamS. WA, Naqvi (2016) An insight into subterranean flow proposition around Alleppey mudbank coastal sector, Kerala, India: inferences from the subsurface profiles of ground penetrating Radar. Environ Earth Sci 75:1361. https://doi.org/10.1007/s12665-016-6172-6

MacPherson H, Kurup PG (1981) Wave damping at the Kerala mudbanks. Indian J Mar Sci 10:154e160. http://nopr.niscair.res.in/handle/123456789/39066

Maher BA (1988) Magnetic properties of some synthetic sub-micron magnetites. Geophys J 94:83–96. https://doi.org/10.1111/j.1365-246X.1988.tb03429.x

Maher BA, Thompson R (eds) (1999) Quaternary climates, environments and magnetism. Cambridge University Press, Cambridge

Mallik TK, Mukherji KK, Ramachandran KK (1988) Sedimentology of the Kerala mud banks (fluid muds?). Mar Geol 80(1–2):99–118. https://doi.org/10.1016/0025-3227(88)90074-6 **(ISSN 0025–3227)**

Mathew J (1992) Wave-mud Interaction in Mudbanks, PhD Thesis. Cochin University of Science and Technology, Cochin, pp 132

Mathew KJ, Gopinathan CP (2000) Study of mud banks of the Kerala coast a retrospect. Marine Fisheries Research and Management, CMFRI, Kochi, pp 117–189. http://eprints.cmfri.org.in/id/eprint/4214

McBride RA, Taylor MJ, Byrnes MR (2007) Coastal morphodynamics and Chenier-Plain evolution in southwestern Louisiana, USA: a geomorphic model. Geomorphology 88(3–4):367–422

Mead AA, Michael TL (2004) Sediment exchange between Amazon mudbanks and shore-fringing mangroves in French Guiana. Mar Geol 208:169–190. https://doi.org/10.1016/j.margeo.2004.04.026

Mehta N, Haluck R, Frecker M (2002) Sequence and task analysis of instrument use in common laparoscopic procedures. Surg Endosc 16:280. https://doi.org/10.1007/s004640080009

Menon KPP (1924) A history of Kerala, vol. 1. Cochin Govt. Press, Cochin, pp 562

Muraleedharan KR, Kumar PKD, Kumar SP (2017) Formation mechanism of mud bank along the Southwest Coast of India. Estuaries Coasts https://doi.org/10.1007/s12237-017-0340-0

Nair RR (1976) Unique mud banks, Kerala, Southwest India: geologic notes. AAPG Bull 60:616–621

Nair RR, Murty PSN (1968) Clay mineralogy of the mud banks of Cochin. Curr Sci India 37(20):589–590

Nair PN, Radhakrishnan, Gopinathan CP, Balachandran VK, Mathew KJ, Regunathan A, Rao DS, Murty AVS (1984) Ecology of mudbanks—phytoplankton productivity in Alleppey mudbank. CMFRI Bull 31:28–35. http://eprints.cmfri.org.in/id/eprint/772

Nair SM, Balchand AN, Peter KJP, Gopinath A (2013) Phenomenal changes in the forms of nitrogen: results from a coastal zone of south west India. Chem Speciat Bioavailab 25:89–96. https://doi.org/10.3184/095422913X137044397727748 **(Taylor and Francis)**

Narayana AC, Priju CP, Chakrabarti A (2001) Identification of a palaeodelta near the mouth of Periyar River in Central Kerala. Geol Soc India 57(6):545–547

Narayana AC, Jago CF, Manojkumar P, Tatavarti R (2008) Nearshore sediment characteristics and formation of mudbanks along the Kerala coast, southwest India. Estuar, Coast Shelf Sci 78(2):341–352, https://doi.org/10.1016/j.ecss.2007.12.012 **(ISSN 0272–7714)**

Nguyen TTH, Zhang W, Li Z, Li J, Ge C, Liu J, Bai X, Feng H, Yu L (2016) Magnetic properties of sediments of the Red River: effect of sorting on the source-to-sink pathway and its implications for environmental reconstruction. Geochem Geophys Geosyst 17: 270–281. https://doi.org/10.1002/2015GC006089

Oldfield F, Yu L (1994) The influence of particle size variations on the magnetic properties of sediments from the northeastern Irish Sea. Sedimentology 41:1093–1108. https://doi.org/10.1111/j.1365-3091.1994.tb01443.x

Oldfield F, Maher BA, Donoghue J, Pierce J (1985) Particle-size related, mineral magnetic source sediment linkages in the Rhode River catchment, Maryland, USA. J Geol Soc 142:1035–1046. https://doi.org/10.1144/gsjgs.142.6.1035

Padmalal D, Kumaran KPN, Nair KM, Ruta B, Limaye S, Vishnu Mohan B, Baijulal S, Anooja (2014) Consequences of sea level and climate changes on the morphodynamics of a tropical coastal lagoon during Holocene: an evolutionary model. Quat Int 333:156–172. https://doi.org/10.1016/j.quaint.2013.12.018 **(ISSN 1040–6182)**

Peterson CD, Komar PD, Scheidegger KF (1986) Distribution, geometry, and origin of heavy mineral placer deposits on Oregon beaches. J Sediment Res 56:67–77. https://doi.org/10.1306/212f8887-2b24-11d7-8648000102c1865d

Purandara BK (1990) Provenance, sedimentation and geochemistry of the modern sediments of the mud banks off the central Kerala coast, India. http://hdl.handle.net/10603/12980

Rahman R, Plater AJ (2014) Particle-size evidence of estuary evolution: a rapid and diagnostic tool for determining the nature of recent saltmarsh accretion. Geomorphology 213:139–152. https://doi.org/10.1016/j.geomorph.2014.01.004

Ramasastry AA, Myrland P (1959) Distribution of temperature, salinity and density in the Arabian sea along the South Malabar coast (South India) during the post-monsoon season. Indian J Fish 6(2):223–255. http://eprints.cmfri.org.in/id/eprint/1872

Randolph A, McBride MJ, Taylor MR, Byrnes (2007) Coastal morphodynamics and Chenier-Plain evolution in southwestern Louisiana, USA: a geomorphic model. Geomorphology 88(3–4):367–422 **(ISSN 0169-555X)**. https://doi.org/10.1016/j.geomorph.2006.11.013

Rine JM, Ginsburg RN (1978) A cyclic sedimentary sequence created by migrating mud banks on an open Holocene shelf, Suriname. Geol Soc Am Bull 10:478

Rine JM, Ginsburg RN (1985) Depositional facies of a mud shoreface in Suriname, South America—a mud analogue to sandy, shallow-marine deposits. J Sediment Res 55(5)

Roberts AP(1995) Magnetic properties of sedimentary greigite (Fe3S4). Earth Planet Sci Lett 134(3–4):227–236. https://doi.org/10.1016/0012-821X(95)00131-U **(ISSN 0012-821X)**

Roberts AP (2015) Magnetic mineral diagenesis. Earth-Sci Rev 151:1–47 https://doi.org/10.1016/j.earscirev.2015.09.010 **(ISSN 0012–8252)**

Roberts AP, Turner GM (1993) Diagenetic formation of ferrimagnetic iron sulphide minerals in rapidly deposited marine sediments, South Island, New Zealand. Earth Planet Sci Lett 115(1–4):257–273. https://doi.org/10.1016/0012-821X(93)90226-Y **(ISSN 0012-821X)**

Rubina R, Plater AJ (2014) Particle-size evidence of estuary evolution: a rapid and diagnostic tool for determining the nature of

recent saltmarsh accretion. Geomorphology 213:139–152. https://doi.org/10.1016/j.geomorph.2014.01.004 **(ISSN 0169-555X)**
Samiksha SV, Vethamony P, Erick Rogers W, Pednekar PS, Babu MT, Dineshkumar PK (2017) Wave energy dissipation due to mudbanks formed off southwest coast of India. Estuar Coast Shelf Sci 196:387–398. https://doi.org/10.1016/j.ecss.2017.07.018 **(ISSN 0272–7714)**
Shynu R, Purnachandra Rao V, Samiksha SV, Vethamony P, Naqvi SWA, Kessarkar PM, Babu MT, Dineshkumar PK (2017) Suspended matter and fluid mud off Alleppey, southwest coast of India. Estuar Coast Sci 185:31–43. https://doi.org/10.1016/j.ecss.2016.11.023 **(ISSN 0272–7714)**
Slingerland Rudy L (1977) The effects of entrainment on the hydraulic equivalence relationships of light and heavy minerals in sands J Sediment Petrol 47(2):753–770. https://doi.org/10.1306/212F7243-2B24-11D7-8648000102C1865D
Snowball IF (1993) Geochemical control of magnetite dissolution in subarctic lake sediments and the implications for environmental magnetism. J Quat Sci 8:339–346. https://doi.org/10.1002/jqs.3390080405
Tamura T, Horaguchi K, Saito Y, Nguyen VL, Tateishi M, OanhTa TK, Nanayama F, Watanabe K (2010) Monsoon-influenced variations in morphology and sediment of a mesotidal beach on the Mekong River delta coast. Geomorphology 116:11–23
Tatavarti R, Narayana AC(2006). Hydrodynamics in a mud bank regime during nonmonsoon and monsoon seasons. J Coastal Res. https://doi.org/10.2112/05-0461.1
Tatavarti R, Narayana A, Ravishankar M, Kumar P (1996) Mudbank dynamics: field evidence of edge waves and far infra-gravity waves. Curr Sci 70(9):837–843. Retrieved from http://www.jstor.org/stable/24099935
Tatavarti R, Narayana AC, Kumar PM (1999) Mudbank regime off the Kerala coast during monsoon and non-monsoon seasons. Proc Indian Acad Sci (Earth Planet Sci) 108:57. https://doi.org/10.1007/BF02840825
Thompson PKR (1986) Seasonal distribution of cyclopoid copepods of the mudbanks off Allepey. Kerala Coast J Mar Biol Assoc 28(1–2):48–56
Thompson R, Oldfield F (1986) Environmental magnetism. Allen and Unwin, London, pp 227. https://doi.org/10.1007/978-94-011-8036-8
Thornton EB, Guza RT (1983) Transformation of wave height distribution. J Geophys Res 88(C10):5925–5938. https://doi.org/10.1029/JC088iC10p05925
Toru T, Keishi H, Yoshiki S, Van LN, Masaaki T, Thi KOT, Futoshi N, Kazuaki W (2010) Monsoon-influenced variations in morphology and sediment of a mesotidal beach on the Mekong River delta coast. Geomorphology 116(1–2):11–23. https://doi.org/10.1016/j.geomorph.2009.10.003 **(ISSN 0169-555X)**
Varadarajan K, Balakrishnan MK (1980) Kerala coast: a landsat's view. Proc Sym Geol Geomorphol Kerala, Spl Publ (5):67–68
Varma PU, Kurup PG (1969) Formation of the Chakara (mudbank) on the Kerala coast. Curr Sci 38:559–560
Walsh JP, Nittrouer CA (2004) Mangrove-bank sedimentation in a mesotidal environment with large sediment supply, Gulf of Papua. Mar Geol 208(2–4):225–248. https://doi.org/10.1016/j.margeo.2004.04.010 **(ISSN 0025-3227)**
Wells JT (1978) Shallow-water waves and fluid-mud dynamics, coast of surinam, South America (No. TR-257). Louisiana State Univ., Coastal Studies Inst., Baton Rouge
Wells JT, Coleman JM (1981a) Physical processes and fine grained sediment dynamics, coast of Surinam, South America. J Sed Petrol 51(4):1053–1068
Wells JT, Coleman JM (1981b) Periodic mud flat progradation, northeastern coast of South America: a hypothesis. J Sediment Petrol 51(4):1069–1075
Wells JT, Roberts HH (1980a) Fluid mud dynamics and shoreline stabilization: Louisiana Chenier Plain. In: 17th International conference on coastal engineering, 23–28 March, 1980, Sydney, Australia. https://doi.org/10.1061/9780872622647.084
Wells JT, Roberts HH (1980b) Fluid mud dynamics and shoreline stabilization: Louisiana chenier plain. Coast Eng 1980:1382–1401
Zhang S, Cioppa MT, Zhang S (2010) Spatial variation in particle size and magnetite concentration on Cedar Beach: implications for grain sorting processes, western Lake Erie, Canada. Dizhi Xuebao 84:1520–1532. https://doi.org/10.1111/j.1755-6724.2010.00345.x